



## 4-Quinazolinyl-oxy-diaryl ureas as novel BRAF<sup>V600E</sup> inhibitors

Mark W. Holladay<sup>a,\*</sup>, Brian T. Campbell<sup>a</sup>, Martin W. Rowbottom<sup>a</sup>, Qi Chao<sup>a</sup>, Kelly G. Sprankle<sup>a</sup>, Andiliy G. Lai<sup>a</sup>, Sunny Abraham<sup>a</sup>, Eduardo Setti<sup>b</sup>, Raffaella Faraoni<sup>a</sup>, Lan Tran<sup>a</sup>, Robert C. Armstrong<sup>a</sup>, Ruwanthi N. Gunawardane<sup>a</sup>, Michael F. Gardner<sup>a</sup>, Merryl D. Cramer<sup>a</sup>, Dana Gitnick<sup>a</sup>, Mark A. Ator<sup>b</sup>, Bruce D. Dorsey<sup>b</sup>, Bruce R. Ruggeri<sup>b</sup>, Michael Williams<sup>b</sup>, Shripad S. Bhagwat<sup>a</sup>, Joyce James<sup>a</sup>

<sup>a</sup> Ambit Biosciences Corporation, 4215 Sorrento Valley Boulevard, San Diego, CA 92121, USA

<sup>b</sup> Cephalon, Inc., 145 Brandywine Parkway, West Chester, PA 19380, USA

### ARTICLE INFO

#### Article history:

Received 28 April 2011

Revised 30 June 2011

Accepted 6 July 2011

Available online 14 July 2011

#### Keywords:

BRAF kinase

Xenograft model

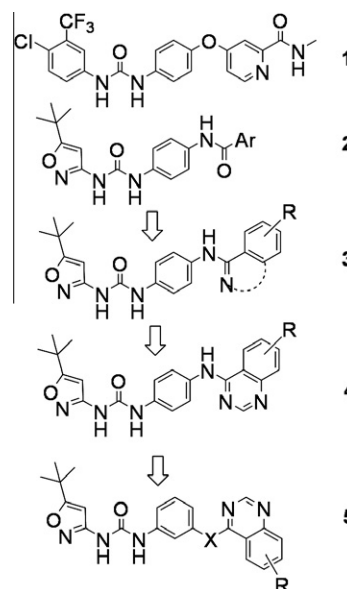
### ABSTRACT

Aryl phenyl ureas with a 4-quinazolinyl-oxy substituent at the meta-position of the phenyl ring are potent inhibitors of mutant and wild type BRAF kinase. Compound **7** (1-(5-tert-butylisoxazol-3-yl)-3-(3-(6,7-dimethoxyquinazolin-4-yloxy)phenyl)urea hydrochloride) exhibits good pharmacokinetic properties in rat and mouse and is efficacious in a mouse tumor xenograft model following oral dosing.

© 2011 Elsevier Ltd. All rights reserved.

The RAS-RAF-MEK-ERK pathway plays a central role in transduction of mitogen and growth factor-initiated signals from the cell surface to the nucleus, thereby modulating key cellular functions including cell growth, proliferation, motility, and survival.<sup>1</sup> The RAF proteins (ARAF, BRAF, and RAF1) are serine/threonine kinases that catalyze phosphorylation of MEK, a downstream serine/threonine kinase in this pathway. Point mutation of the BRAF Val-600 residue to Glu (BRAF<sup>V600E</sup>) results in constitutive activation of BRAF, and hence constitutive activation of the RAS-RAF-MEK-ERK pathway.<sup>2</sup> Mutated BRAF is found in 55–68% of melanomas, 29–83% of papillary thyroid tumors, and 4–16% of colorectal cancers, among others, and is a key factor in the uncontrolled proliferation of these tumors.<sup>3–5</sup> Drug discovery efforts directed toward inhibitors of BRAF and related family members have resulted in the identification of sorafenib (Nexavar<sup>TM</sup>, **1**, Fig. 1), a marketed agent for renal cell and hepatocellular carcinomas. Sorafenib exhibits potent pan-VEGF-R activity, and it is hypothesized that this mechanism of action substantially contributes to the observed clinical effects. Other agents targeting BRAF<sup>V600E</sup> including RAF-265 and PLX-4032 are undergoing clinical evaluation,<sup>1,6</sup> with significant clinical benefit having been recently reported for PLX-4032.<sup>7</sup>

We have described previously a series of amide-substituted 5-*t*-butyl-3-isoxazolyl phenyl ureas **2** (Fig. 1) as potent FLT3 inhibitors.<sup>8</sup> Through application of Ambit's KINOMEScan<sup>TM</sup> platform,<sup>9</sup> activity against BRAF<sup>V600E</sup> was recognized in some analogs of the series represented by **2**. Further elaboration around **2** included

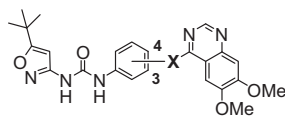


**Figure 1.** Structure of sorafenib (**1**) and evolution of the 4-quinazolinyl-oxy-diaryl urea series of BRAF inhibitors.

incorporation of the amide carbonyl oxygen (as nitrogen) into a ring fused to the adjacent aryl moiety (cf. structure **3**), leading eventually to quinazolines **4**. Certain *meta*-substituted variants of **2** and **4** were observed to show superior activity against BRAF,

\* Corresponding author. Tel.: +1 858 334 2141.

E-mail address: mholladay@ambitbio.com (M.W. Holladay).

**Table 1**  
Effect of linker X on properties of BRAF inhibitors

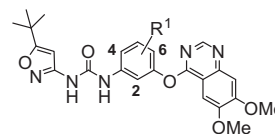
Cmpd	X	BRAF <sup>V600E</sup> K <sub>d</sub> (nM) <sup>a</sup>	A375 pMEK IC <sub>50</sub> (nM) <sup>a</sup>	S <sub>10</sub>	%F <sup>b</sup>
<b>1</b>	–	284	6599	0.16	–
<b>6</b>	3-NH	40 (4)	82 (5)	0.10	1.9
<b>7</b>	3-O	73 (20)	121 (20)	0.29	49
<b>8</b>	3-S	61 (4)	118 (6)	0.18	24
<b>9</b>	4-NH	478 (4)	–	0.30	<1

<sup>a</sup> Average value, with number of determinations shown in parentheses.<sup>b</sup> Dosed as hydrochloride salt in rats unless otherwise indicated.

leading to the series represented by **5**. Herein we describe the SAR around structure **5** with respect to binding affinity ( $K_d$ ) to BRAF<sup>V600E</sup> and potency (IC<sub>50</sub>) to inhibit BRAF<sup>V600E</sup>-dependent MEK phosphorylation in A375 cells. A previous letter from these laboratories described a selectivity score ( $S$ ) as a preliminary indicator of specificity across the human kinome.<sup>9</sup> In the present letter, an  $S_{10}$  score represents the fraction of 290 kinases tested that show <10% activity (>90% inhibition) compared to control at a 10  $\mu$ M screening concentration. Pharmacokinetic assessments played a significant role in guiding the SAR in this series, and therefore oral bioavailability in rat is reported for selected analogs. Finally, efficacy in a mouse tumor xenograft model is disclosed for three leading analogs identified from these studies.

Table 1 shows the effect of various linkers X on BRAF<sup>V600E</sup> inhibition and other key properties. Among compounds linked to quinazoline through the *meta*-position of the central phenylene ring, NH-, O-, and S-linked compounds (**6–8**) all showed potent binding affinity (40–73 nM) and cell activity (82–121 nM). The  $S_{10}$  scores of these analogs followed the order NH<S<O, that is, the *meta*-O analog showed the least kinome specificity among this set. Consistent with the SAR described above, compound **9**, having the *para*-NH-linker, showed markedly lower binding affinity for BRAF<sup>V600E</sup> than the corresponding *meta*-NH linked compound **6**. Compound **9** also showed substantially lower kinome specificity (higher  $S_{10}$  score) than **6**.

Although the binding affinity, cell potency, and kinome specificity of compound **6** were attractive, this analog showed inferior pharmacokinetic (PK) properties in rats compared to the corresponding *meta*-O- and *meta*-S-linked compounds. This pattern of

**Table 3**  
Effect of central phenyl ring substitutions on properties of BRAF inhibitors

Cmpd	R <sup>1</sup>	BRAF <sup>V600E</sup> K <sub>d</sub> (nM) <sup>a</sup>	A375 pMEK IC <sub>50</sub> (nM) <sup>a</sup>	S <sub>10</sub>	%F <sup>b</sup>
<b>17</b>	2-Me	38 (2)	179 (2)	0.30	–
<b>18</b>	4-F	56 (2)	113 (2)	0.38	–
<b>19</b>	4-Cl	99 (2)	229 (2)	0.24	–
<b>20</b>	6-F	72 (2)	62 (4)	0.31	22
<b>21</b>	4,6-di-F	46 (2)	113 (2)	0.37	14 <sup>c</sup>

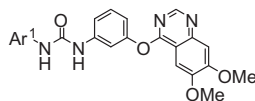
<sup>a,b</sup> Same as Table 1.<sup>c</sup> Dosed as free base.

inferior PK properties for *meta*-NH-linked compounds persisted across numerous analogs that were prepared with all three (NH-, O-, and S-) linkers (data not shown). The remainder of this letter will focus on analogs having a *meta*-O-linker between the quinazoline moiety and the central phenyl ring, with compound **7** as the prototype.

Table 2 shows the properties of compounds with Ar<sup>1</sup> = phenyl or substituted phenyl. The unsubstituted phenyl analog **10** was markedly less potent than **7** in both binding and cell assays, whereas a number of phenyl substitution patterns afforded analogs with binding affinities comparable to that of **7**. On the other hand, there was a trend toward modest to significantly reduced cell potency across this series of analogs. For example, compound **16** (which has the same phenyl substitution pattern as sorafenib **1**) showed similar binding affinity to that of **7** but nearly six-fold lower cell potency. These analogs also generally exhibited higher kinome specificity than that of **7**.

The effects of conservative substitutions on the central phenyl ring of compound **7** are shown in Table 3. In general, these modifications were well tolerated, but did not appear to afford any particular advantage to the profiles of these compounds.

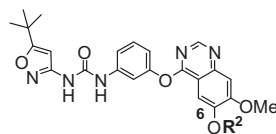
Tables 4 and 5 show, respectively, the effects of replacing the methoxy group on either the 6- or 7-position of the quinazoline ring with hydroxy, ethoxy, methoxyethoxy, or an aminoalkoxy group. In general, these modifications were well tolerated with respect to binding affinity, consistent with a hypothesis that this region of the molecule extends outside the catalytic cleft toward solvent. These changes also are consistent with potent cell activity,

**Table 2**  
Effect of Ar<sup>1</sup> moiety on properties of BRAF inhibitors

Cmpd	Ar <sup>1</sup>	BRAF <sup>V600E</sup> K <sub>d</sub> (nM) <sup>a</sup>	A375 pMEK IC <sub>50</sub> (nM) <sup>a</sup>	S <sub>10</sub>	%F
<b>10</b>	Ph	370 (2)	>15000 (2)	0.09	–
<b>11</b>	3-CF <sub>3</sub> -Ph	46 (2)	1664 (2)	0.18	–
<b>12</b>	3- <i>t</i> -Bu-Ph	36 (2)	333 (2)	0.18	–
<b>13</b>	3-MeO-Ph	90 (2)	ca. 10000 (2)	0.10	–
<b>14</b>	4-Cl-Ph	30 (2)	1850 (2)	0.15	–
<b>15</b>	4- <i>t</i> -Bu-Ph	96 (2)	290 (2)	0.17	15 <sup>b</sup>
<b>16</b>	3-CF <sub>3</sub> -4-Cl-Ph	98 (2)	696 (2)	0.16	–

<sup>a</sup> Same as Table 1.<sup>b</sup> Dosed as free base.

**Table 4**  
Effect of modifications at the 6-position of the quinazoline ring on properties of BRAF inhibitors

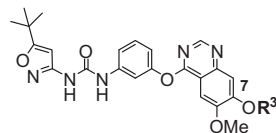


Cmpd	R <sup>2</sup>	BRAF <sup>V600E</sup> K <sub>d</sub> (nM) <sup>a</sup>	A375 pMEK IC <sub>50</sub> (nM) <sup>a</sup>	S <sub>10</sub>	%F <sup>b</sup>
<b>22</b>	H	46 (2)	86 (4)	0.24	–
<b>23</b>	Et	67 (4)	80 (4)	0.28	30 (2)
<b>24</b>	-(CH <sub>2</sub> ) <sub>2</sub> Ome	48 (2)	59 (2)	0.26	13
<b>25</b>	-(CH <sub>2</sub> ) <sub>2</sub> -4-morpholinyl	38 (2)	52 (4)	0.28	11 <sup>c</sup>
<b>26</b>	-(CH <sub>2</sub> ) <sub>3</sub> -4-morpholinyl	29 (2)	36 (4)	0.30	20
<b>27</b>	-(CH <sub>2</sub> ) <sub>2</sub> -1-piperidinyl	96 (2)	293 (2)	0.25	–

<sup>a,b</sup> Same as Table 1.

<sup>c</sup> Dosed as free base.

**Table 5**  
Effect of modifications at the 7-position of the quinazoline ring on properties of BRAF inhibitors



Cmpd	R <sup>3</sup>	BRAF <sup>V600E</sup> K <sub>d</sub> (nM) <sup>a</sup>	A375 pMEK IC <sub>50</sub> (nM) <sup>a</sup>	S <sub>10</sub>	%F <sup>b</sup>
<b>28</b>	H	57 (2)	110 (4)	0.20	<1 <sup>c</sup>
<b>29</b>	Et	82 (2)	173 (4)	0.29	16
<b>30</b>	-(CH <sub>2</sub> ) <sub>2</sub> Ome	57 (8)	100 (12)	0.31	56
<b>31</b>	-(CH <sub>2</sub> ) <sub>2</sub> -4-morpholinyl	34 (2)	165 (8)	0.27	52 <sup>c</sup>
<b>32</b>	-(CH <sub>2</sub> ) <sub>3</sub> -4-morpholinyl	56 (2)	96 (4)	0.35	18 <sup>c</sup>

<sup>a,b</sup> Same as Table 1.

<sup>c</sup> Dosed as free base.

with a number of variants exhibiting cellular potency in the mid-double digit nanomolar range. In general, these modifications did not result in meaningful alterations in the kinase specificities of these molecules. In many cases, bioavailabilities were less favorable after incorporation of solubilizing groups, although compounds **30** and **31** showed bioavailabilities comparable to that of compound **7**.

When plasma clearance was determined from iv studies, values for most of the analogs in Tables 4 and 5 bearing solubilizing groups were higher than that of **7**, consistent with the likelihood of a significant first pass clearance, although compounds **30** and **31** showed lower iv clearance values than that of **7**.

Compounds **7**, **8**, and **31** were further evaluated in pharmacokinetic and antitumor efficacy studies. Good plasma exposure was observed for all three compounds upon oral administration to mice [cmpd; dose (mg/kg); plasma AUC (μM × h)]: [**7**; 30; 12.5]; [**8**; 30; 22]; [**31**; 100; 48]. Oral administration of **7** to mice bearing Colo-205 tumors at 100 mg/kg bid resulted in sustained tumor stasis throughout the dosing period (Fig. 2), which included a 55% incidence of tumor regressions. Compound **8** at 55 mg/kg or 100 mg/kg showed tumor stasis early in the dosing period, accompanied by significant tumor regrowth before the end of the dosing period (see Supplementary data). Interestingly, by day 8, efficacy was notably inferior at the higher dose of compound **8**. Compound **31** at 100 mg/kg bid exhibited a maximum 65% tumor growth inhibition, also accompanied by tumor regrowth before the end of the dosing period (see Supplementary data). No body weight loss

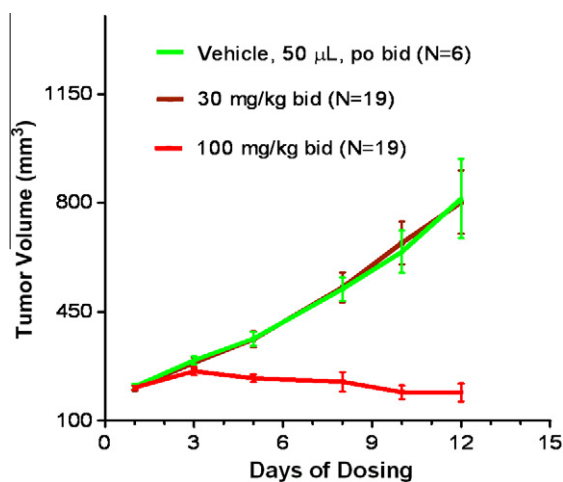
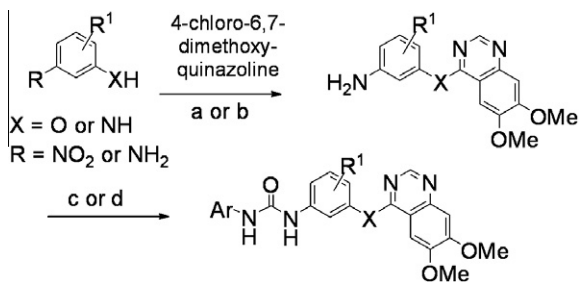
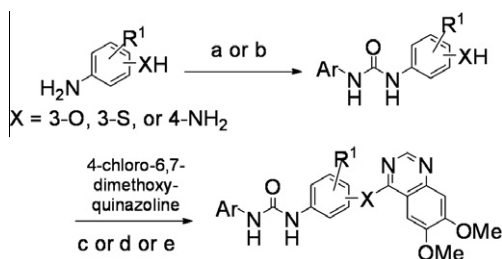


**Figure 2.** Antitumor efficacy of orally administered compound **7** in the mouse Colo-205 tumor xenograft model. Statistical significance relative to vehicle controls: 30 mg/kg bid group: NS; 100 mg/kg bid group: days 5–8,  $p < 0.0004$ ; days 10–12 (termination of dosing),  $p < 0.0002$ .

was observed for **8** or **31**, whereas **7** showed 8% maximum body weight loss that was reversible following cessation of compound administration. On day 5 of dosing, all three compounds at 100 mg/kg bid showed  $\geq 50\%$  reduction in levels of phosphorylated



**Scheme 1.** Reagents and conditions: (a) (R = NH<sub>2</sub>) Cs<sub>2</sub>CO<sub>3</sub>, THF, 50 °C; (b) (R = NO<sub>2</sub>) (i) KOtBu, DMA, 150 °C; (ii) H<sub>2</sub>, Pd-C, MeOH; (c) ArNCO, THF or DMF, rt – 80 °C; (d) Ar-NHCO<sub>2</sub>Ph, THF, NEt<sub>3</sub>, DMAP, 50–80 °C.

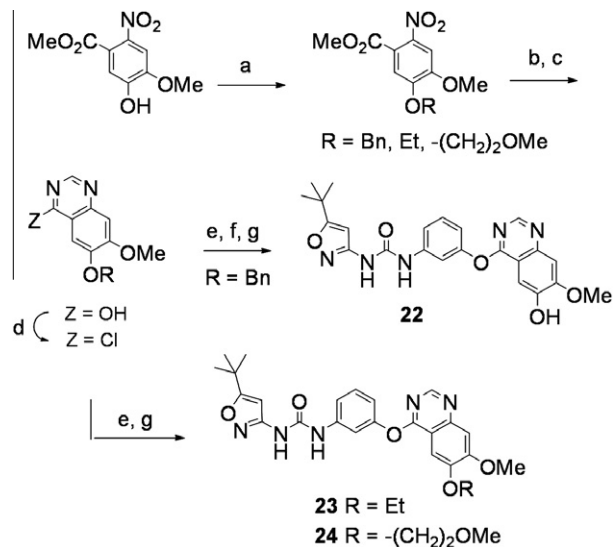


**Scheme 2.** Reagents and conditions: (a) ArNCO, THF or PhMe or DMF, optional NEt<sub>3</sub>, 50–70 °C; (b) ArNHCO<sub>2</sub>Ph, CH<sub>3</sub>CN, DBU, 50 °C; (c) (X = 3-O) KOtBu or Cs<sub>2</sub>CO<sub>3</sub>, optional K<sub>2</sub>CO<sub>3</sub> or NEt<sub>3</sub>, THF or DMF, rt – 80 °C; (d) (X = 3-S) NaH, THF, rt – 50 °C; (e) (X = 4-NH) *n*-BuOH, reflux.

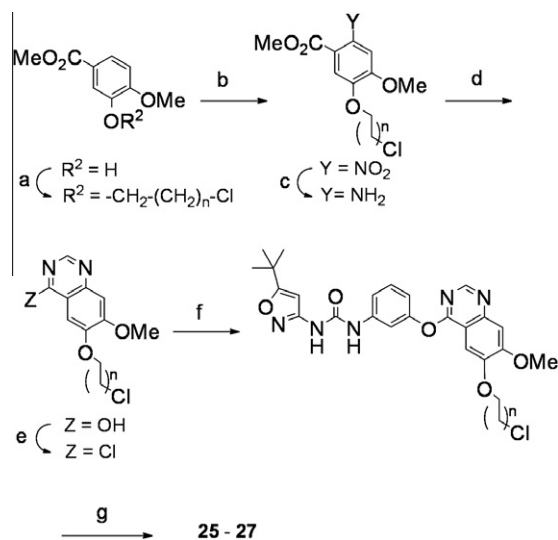
MEK (pMEK) in tumor tissue at 10 h post-dose (see [Supplementary data](#)). Given comparable cellular potencies among **7**, **8**, and **31**, together with similar or better single dose exposure and pMEK suppression for **8** and **31** as compared with **7**, the observation of overall inferior antitumor activity observed for **8** and **31** merits comment. We note that the greatest differences in antitumor behavior among the compounds first become apparent about 8 days after the start of dosing, which is several days after the above pharmacokinetic and pharmacodynamic readings were taken. We speculate that differential changes in metabolism or distribution of the compounds, for example as a result of differential induction of metabolizing enzymes or transporter molecules, may have become manifest by this later time. The reverse dose-response relationship observed for **8** in vivo might furthermore be a consequence of a propensity for this compound to induce such effects. We do not believe that potential differences in kinase specificity among the compounds offers a likely explanation for the disparate in vivo behaviors observed, since review of the kinase inhibition profiles indicated that any additional kinases significantly inhibited by **7** were similarly inhibited by at least one of, and usually both of, **8** and **31**.

Schemes 1–4 illustrate representative synthetic routes to key compounds described in this letter. Compounds **28–32** (quinazolinone 7-position modifications, [Table 5](#)) were prepared using methods analogous to those described in Schemes 3 and 4 for quinazolinone 6-position modifications ([Table 4](#)) using the appropriate regioisomeric starting materials.

In summary, quinazolinone-diaryl ureas and structurally related analogs were synthesized and evaluated as inhibitors of BRAF, and analogs with favorable potency, kinase specificity, and pharmacokinetic profiles were identified. In a mouse xenograft model, compound **7** exhibited sustained antitumor efficacy (stasis with regressions) accompanied by a pharmacodynamic readout for BRAF inhibition at a dose that induced minimal body weight loss. Further optimization of this series will be reported in due course.



**Scheme 3.** Reagents and conditions: (a) alkyl halide, KI, K<sub>2</sub>CO<sub>3</sub>, DMF, 90–95 °C; (b) Na<sub>2</sub>S<sub>2</sub>O<sub>4</sub>, MeOH, H<sub>2</sub>O, 55 °C; (c) HCONH<sub>2</sub>, HOAc, 130 °C; (d) POCl<sub>3</sub>, 110–115 °C; (e) 3-aminophenol, Cs<sub>2</sub>CO<sub>3</sub>, THF, 75 °C, 25 h; (f) H<sub>2</sub>, Pd-C, EtOH/THF, 50–55 °C; (g) Ar-NHCO<sub>2</sub>Ph, DMF, 60 °C.



**Scheme 4.** Reagents and conditions: (a) Br(CH<sub>2</sub>)<sub>n</sub>CH<sub>2</sub>Cl, K<sub>2</sub>CO<sub>3</sub>, DMF, rt – 60 °C; (b) HNO<sub>3</sub>, Ac<sub>2</sub>O, HOAc, 50 °C; (c) H<sub>2</sub>, Pd-C, EtOAc; (d) formamidinium-HCl, EtOH, sealed tube 130 °C; (e) POCl<sub>3</sub>, NEt<sub>3</sub>, 100 °C; (f) Ar-NH(CO)NH-C<sub>6</sub>H<sub>4</sub>-m-OH, KOtBu or Cs<sub>2</sub>CO<sub>3</sub>, optional K<sub>2</sub>CO<sub>3</sub> or NEt<sub>3</sub>, THF or DMF, rt – 80 °C; (g) 2° amine, *n*-Bu<sub>4</sub>Ni, NEt<sub>3</sub>, DMF, 60 °C, 2–3 d.

## Acknowledgments

We are grateful to the Ambit KINOMEScan™ team for generating BRAF<sup>V600E</sup> K<sub>d</sub> values and S<sub>10</sub> scores and to Ianina Valenta for her contributions to generating data from cellular assays.

## Supplementary data

Supplementary data (synthetic details for preparation of compounds **7**, **8**, and **31**, a table summarizing antitumor and pharmacodynamic data from mouse tumor xenograft studies for compounds **7**, **8**, and **31**, and the antitumor efficacy results in graphical form for compounds **8** and **31** are included) associated

with this article can be found, in the online version, at [doi:10.1016/j.bmcl.2011.07.019](https://doi.org/10.1016/j.bmcl.2011.07.019).

### References and notes

1. Roberts, P. J.; Der, C. J. *Oncogene* **2007**, *26*, 3291.
2. Michaloglou, C.; Vredeveld, L. C.; Mooi, W. J.; Peeper, D. S. *Oncogene* **2007**, *27*, 1.
3. Beeram, M.; Patnaik, A.; Rowinsky, E. K. *J. Clin. Oncol.* **2005**, *23*, 6771.
4. Haluska, F. G.; Tsao, H.; Wu, H.; Haluska, F. S.; Lazar, A.; Goel, V. *Clin. Cancer Res.* **2006**, *12*, 2301s.
5. Ouyang, B.; Knauf, J. A.; Smith, E. P.; Zhang, L.; Ramsey, T.; Yusuff, N.; Batt, D.; Fagin, J. A. *Clin. Cancer Res.* **2006**, *12*, 1785.
6. Hersey, P.; Bastholt, L.; Chiarion-Sileni, V.; Cinat, G.; Dummer, R.; Eggermont, A. M. M.; Espinosa, E.; Hauschild, A.; Quirt, I.; Robert, C.; Schadendorf, D. *Ann. Oncol.* **2009**, *20*, vi35.
7. Garber, K. *Science* **2009**, *326*, 619.
8. Patel, H. K.; Grotzfeld, R. M.; Lai, A. G.; Mehta, S. A.; Milanov, Z. V.; Chao, Q.; Sprankle, K. G.; Carter, T. A.; Velasco, A. M.; Fabian, M. A.; James, J.; Treiber, D. K.; Lockhart, D. J.; Zarrinkar, P. P.; Bhagwat, S. S. *Bioorg. Med. Chem. Lett.* **2009**, 5182.
9. Karaman, M. W.; Herrgard, S.; Treiber, D. K.; Gallant, P.; Atteridge, C. E.; Campbell, B. T.; Chan, K. W.; Ciceri, P.; Davis, M. I.; Edeen, P. T.; Faraoni, R.; Floyd, M.; Hunt, J. P.; Lockhart, D. J.; Milanov, Z. V.; Morrison, M. J.; Pallares, G.; K Patel, H.; Pritchard, S.; Wodicka, L. M.; P Zarrinkar, P. *Nat. Biotechnol.* **2008**, *26*, 27.